agronomy

MDPI

Article

Effects of Biochar and Its Fractions on Soil Nitrogen Forms and Microbial Communities Under Freeze-Thaw Conditions

Xiaoyuan Gao [1], Yunfei Wang [2], Ming Li [1], Jie Yu [3,*] and Song Han [1,*]

[1] College of Forestry, Northeast Forestry University, Harbin 150040, China; 2022020076@nefu.edu.cn (X.G.); liming1986@nefu.edu.cn (M.L.)
[2] College of Environment and Energy, Zhejiang Guangsha Vocational and Technical University, Jinhua 321000, China; 20233613@zjgsdx.edu.cn
[3] Heilongjiang Academy of Black Soil Conservation & Utilization, Harbin 150086, China
* Correspondence: haas_yuki@163.com (J.Y.); songh77@nefu.edu.cn (S.H.)

Abstract

Biochar shows potential for regulating nitrogen cycling in cold-region soils, but the roles of its different fractions during freeze-thaw cycles (FTCs) remain unclear. To elucidate the regulation of cold-region soil environments by biochar at the fraction scale, we examined the effects of biochar and its fractions (dissolved and undissolved) on soil nitrogen forms and microbial communities under simulated FTCs. The experiment included a constant-temperature control, a freeze–thaw control, and three biochar treatments with pristine biochar (PBC), dissolved biochar fraction (DBC), and undissolved biochar fraction (UBC), respectively, maintained in triplicate at five FTC frequencies (0, 1, 5, 10, and 20). Changes in soil physicochemical properties and nitrogen forms were measured at five FTC frequencies, and microbial community composition was analyzed by high-throughput sequencing after the 20th cycle. Both biochar fractions reduced inorganic nitrogen, with ammonium nitrogen decline resulting from joint action and nitrate nitrogen (NO_3^--N) reduction dominated by UBC. PBC alleviated microbial biomass nitrogen stress by relying primarily on its undissolved fraction to enhance soil water retention, organic carbon, and total nitrogen. Redundancy analysis indicated that total nitrogen and NO_3^--N were the key factors affecting microbial community composition. Partial least squares structural equation modeling results suggested that soil physicochemical properties influenced microbial community structure characteristics more strongly than nutrient properties. These findings provide a new perspective on the regulatory mechanism of biochar on the agricultural soil environment in cold regions.

Keywords: cold-region agriculture; biochar fractions; black soil; nitrogen transformation; bacterial community

Academic Editor: Huashou Li

Received: 16 September 2025
Revised: 13 October 2025
Accepted: 15 October 2025
Published: 21 October 2025

Citation: Gao, X.; Wang, Y.; Li, M.; Yu, J.; Han, S. Effects of Biochar and Its Fractions on Soil Nitrogen Forms and Microbial Communities Under Freeze-Thaw Conditions. *Agronomy* **2025**, *15*, 2437. https://doi.org/10.3390/agronomy15102437

1. Introduction

Freeze-thaw cycles (FTCs) are a natural phenomenon that occurs widely in mid- to high-latitude and high-altitude regions around the world. With global warming, soils in cold regions are projected to experience more frequent freeze-thaw events [1,2]. These changes can strongly affect soil structure, microorganisms, nutrient cycling, and ecological functions. Nitrogen, as an essential element for all living organisms, plays a crucial role in sustaining agricultural ecosystem balance through its cycling [3]. FTCs alter the forms and availability of soil nitrogen by disrupting soil physical structure, lysing microbial cells, and damaging fine plant roots [4,5]. The changes in substrate availability induced by FTCs

stimulate microbial metabolism and soil nitrogen cycling processes, thereby increasing the risks of nitrogen loss via leaching or gaseous emissions in agricultural ecosystems [6].

Biochar, as a soil amendment, has exhibited considerable promise in enhancing soil physicochemical properties, regulating soil nutrient cycles, and remediating soil pollution [7]. Due to its physicochemical properties, biochar exerts its regulatory effects on soil environments through multiple complex mechanisms [8]. However, biochar in the environment is not a uniform material; rather, it partitions into freely dissolved and undissolved fractions [9]. The dissolved fraction of biochar is operationally defined as the portion capable of passing through a 0.45-μm filter membrane, which includes soluble salts, minerals, and dissolved organic matter [10]. This fraction exhibits higher polarity and reactivity [11]. In contrast, the undissolved fraction consists of carbon skeletons and insoluble minerals, characterized by greater aromaticity and stability [12,13]. This heterogeneity of structure and molecular composition leads to divergent environmental functions, as demonstrated in processes including heavy metal adsorption [14], mitigation of soil acidification [15], influence on algal growth [16], and promotion of soil carbon sequestration [17]. Moreover, the differences in the regulatory functions of biochar fractions may lead to differential responses in microbial communities by directly changing the soil physicochemical environment (such as pH, pore structure, or nutrient availability) [18]. Therefore, analyzing the differential contributions of biochar fractions to soil environmental regulation can help further elucidate the intricate regulatory mechanisms of biochar on the soil environment.

Previous studies have established that biochar influences soil nitrogen dynamics through several mechanisms, such as retaining ammonium nitrogen and nitrate nitrogen via surface sorption and cation exchange [19,20]; improving water retention to reduce nitrogen leaching and promote microbial assimilation [21,22]; stimulating biological nitrogen fixation by plants and microbes [23]; and regulating microbial nitrogen conversion to reduce N_2O emissions [24]. The disturbance of the soil environment and microbial activity caused by FTCs may interact with the regulatory effect of biochar in complex ways. The potential of biochar to regulate soil nitrogen forms [25,26], nitrogen losses [27,28], and microbial community structure [29] under FTCs has garnered increasing attention. However, these studies primarily treated biochar as a homogeneous entity, ignoring the possibility that its dissolved and undissolved fractions may contribute heterogeneously to the observed effects. The role of biochar fractions in regulating soil nitrogen transformation and microbial ecology under freeze-thaw stress remains unclear. Under frequent freeze-thaw disturbances, the regulation of the soil environment by biochar fractions may cause more complex changes. Thus, analyzing how distinct biochar fractions affect soil nitrogen forms and microbial communities under freeze-thaw conditions is essential to understanding biochar's role in regulating nitrogen cycling in cold regions.

To elucidate the regulation of cold-region soil environments by biochar at the fraction scale, simulated FTC experiments were conducted using soil from the Songnen Plain as the research object, with biochar and its two fractions applied as exogenous amendments. The main objectives of this study were as follows: (1) to elucidate the differential effects of distinct biochar fractions on soil physicochemical properties and nitrogen forms under FTCs and to identify the dominant functional fraction; (2) to investigate the causes of differential responses in soil microbial communities induced by biochar fraction under FTCs. We hypothesized that under freeze-thaw conditions: (1) Biochar fractions could exert differential regulatory effects on soil environmental microbial communities; (2) The undissolved fraction of biochar would provide a greater regulatory effect on nitrogen forms. This study provides novel insights into the mechanisms by which biochar and its fractions regulate nitrogen transformation and microbial responses under FTCs, offering a scientific basis for improving soil fertility and ecological stability in cold-region agricultural systems.

2. Materials and Methods

2.1. Soil Sample

Soil samples were collected from farmland (45°37′ N, 126°46′ E) in Harbin, Heilongjiang Province, China. The soil is classified as Black Soil according to the Chinese Soil Taxonomy, corresponding to Mollisols in the US Soil Taxonomy. The region experiences a temperate continental monsoon climate, with an average annual temperature of 2–5 °C and an average annual rainfall of 400–600 mm. The surface soil (0–20 cm) was air-dried naturally and sieved through a 2 mm sieve to remove gravel, plant roots, and other debris. The basic properties of the test soil are shown in Table 1.

Table 1. The basic properties of the test soil.

Item	Value	Item	Value
pH	6.35	Available P ($mg \cdot kg^{-1}$)	48.92
Electrical conductivity ($\mu S \cdot cm^{-1}$)	162.3	Rapidly available K ($mg \cdot kg^{-1}$)	141.38
Organic matter ($g \cdot kg^{-1}$)	46.74	Sand (%)	16.92
Organic C ($g \cdot kg^{-1}$)	27.11	Silt (%)	58.23
Total N ($g \cdot kg^{-1}$)	1.68	Clay (%)	24.87
Total P ($g \cdot kg^{-1}$)	0.57	Texture (USDA)	Silt Loam
NH_4^+-N ($mg \cdot kg^{-1}$)	17.19	Bulk density ($g \cdot cm^{-3}$)	1.35
NO_3^--N ($mg \cdot kg^{-1}$)	26.67	Water holding capacity (%)	36.50

2.2. Extraction of Biochar Fractions

The corn stover biochar was purchased from Lize Environmental Protection Co., Ltd. (Zhengzhou, China), and was prepared under oxygen-limited conditions at 500–600 °C. The pristine biochar was crushed and sieved through a 60-mesh sieve for later use, denoted as PBC. The extraction of the fractions of biochar was referred to a previous study [15]. In brief, the PBC and deionized water were mixed in a ratio of 1:10 and stirred for 48 h. The obtained suspension passing through the 0.45-μm filter was the dissolved biochar fraction, denoted as DBC. The remaining solid particles were the undissolved biochar fraction, which continued to be rinsed with deionized water until the EC of the filtrate was <50 $\mu S \cdot cm^{-1}$ (i.e., less than 2% of the EC of PBC). Then the undissolved biochar fraction was dried in an oven at 60 °C to a constant weight, denoted as UBC. The basic properties of biochar and its fractions are shown in Table 2.

Table 2. Properties of biochar and its fractions.

Name	pH	EC ($\mu S \cdot cm^{-1}$)	Organic C	Total N	Total P	Total K
Pristine biochar (PBC)	9.12	2690	37.99%	0.64%	0.19%	2.70%
Undissolved biochar fraction (UBC)	9.37	265	43.23%	0.69%	0.12%	1.44%
Dissolved biochar fraction (DBC)	8.97	2760	86.77 $mg \cdot L^{-1}$	1.43 $mg \cdot L^{-1}$	3.17 $mg \cdot L^{-1}$	571.6 $mg \cdot L^{-1}$

2.3. Experimental Design

The incubation experiment included five treatments: (1) constant temperature control soil (CTS), (2) freeze-thaw control soil (FTS), (3) soil with PBC (S + PBC), (4) soil with DBC (S + DBC), and (5) soil with UBC (S + UBC). Each treatment consisted of 15 replicates (5 sampling times × 3 replicates) for a total of 72 samples (samples in the CTS and FTS groups at cycle 0 were the same). A set of PET jars was used as containers for the incubation experiments. In brief, 50 g of soil (dry weight) was mixed with the corresponding biochar fractions. PBC and UBC were applied to the soil at a rate of 2 wt.%. For the DBC treatment,

an amount equivalent to its extraction yield was applied, specifically 10 mL per equivalent unit of soil. The soil moisture content was adjusted to 22% using deionized water via the weighing method, equivalent to 60% WHC. The soil samples were then packed into the jars at a bulk density of 1.35 g/cm^3 and covered with a sealing film to reduce moisture loss. Before the freeze-thaw cycle began, all samples were pre-incubated at 10 °C for 7 days to restore soil microbial activity. During pre-incubations, moisture content was checked and adjusted by weighing every 3 days. No further moisture adjustments were made to the samples after the formal incubation began.

According to the climate characteristics of the Songnen Plain, each freeze-thaw cycle included freezing at −15 °C for 12 h and thawing at 10 °C for 12 h [30], totaling 24 h per freeze-thaw cycle. The CTS group was incubated at 10 °C throughout the experiment period. A total of 20 cycles were performed. Destructive sampling was conducted at 0th, 1st, 5th, 10th, and 20th freeze-thaw cycles (denoted as C0, C1, C5, C10, and C20, respectively). At each sampling time, three replicates from each treatment were randomly collected and mixed for analysis.

2.4. Soil Indexes Determination Methods

2.4.1. Soil Environmental Factors Determination Methods

The reagents used in this study were all purchased from Tianjin Kemiou Chemical Reagent Co., Ltd. (Tianjin, China). Among them, sodium hydroxide (NaOH) and potassium persulfate ($K_2S_2O_8$) were of GR grade; potassium sulfate (K_2SO_4), potassium chloride (KCl), potassium dichromate ($K_2Cr_2O_7$), sulfuric acid (H_2SO_4), and hydrochloric acid (HCl) were of AR grade.

Soil moisture content was determined using the oven-dry method [31]. Soil pH and EC were determined using a pH meter (PHS-3E, Shanghai INESA Scientific Instrument Co., Ltd., Shanghai, China) and conductivity meter (DDS-307A, Shanghai INESA Scientific Instrument Co., Ltd., Shanghai, China), respectively, at a soil:water ratio of 1:5 [32]. Soil available phosphorus (AP) and rapidly available potassium (AK) content were determined by the universal extract-colorimetric method using a UV spectrophotometry (T6 New Century, Beijing Puxi General Instrument Co., Ltd., Beijing, China) with reference to NY/T 1848-2010 [33]. Soil dissolved organic carbon (DOC) was extracted by 0.5 M K_2SO_4 and determined by the potassium dichromate oxidation method [34]. SOC was determined by the potassium dichromate oxidation-spectrophotometric method with reference to HJ 615-2011 [35]. NH_4^+-N and NO_3^--N in soil were extracted with 1 M KCl solution. NH_4^+-N was determined by the indophenol blue colorimetric method with reference to GB/T 42485-2023 [36], and NO_3^--N was determined by UV spectrophotometry with reference to GB/T 32737-2016 [37]. Soil inorganic nitrogen (inorganic N) content was calculated by adding the contents of NH_4^+-N and NO_3^--N. Soil microbial biomass nitrogen (MBN) was determined by the chloroform fumigation-extraction method with reference to GB/T 39228-2020 [38]. Using 0.5 M K_2SO_4 to extract the soil before and after fumigation, the nitrogen content in the leachate was oxidized by alkaline potassium persulfate and determined by UV spectrophotometry. Total nitrogen (total N) was determined by the Kjeldahl method [39] using a semi-automatic Kjeldahl nitrogen analyzer (KDN, Hangzhou Lvbo Instruments Co., Ltd., Hangzhou, China).

2.4.2. High-Throughput Sequencing of Soil Microbial Communities

Fresh soil samples of each group after the 20th cycle were collected for soil microbial community analysis. The specific details of DNA extraction, 16S rRNA gene amplification, and sequencing methods are provided in the Supplementary Materials S1. The raw sequencing data generated in this study have been deposited in the NCBI Se-

quence Read Archive (SRA) under BioProject accession number PRJNA1328359. Bioinformatic analysis of the soil microbiota was carried out using the Majorbio Cloud platform (https://cloud.majorbio.com) (accessed on 27 August 2025). Based on OTU information, alpha diversity indices (including Shannon, Simpson, Ace, and Chao1 indices) were calculated to assess microbial abundance and diversity (Mothur v1.30.1). The Shannon and Simpson indices were used to assess community diversity, while the Ace and Chao1 indices were employed to evaluate community richness. To assess whether significant differences exist in the microbial community structure among different groups, we employed Principal Coordinates Analysis (PCoA) based on the Euclidean distance dissimilarity combined with the ANOSIM test method (Vegan v2.5-3 package). To further identify the microbes driving inter-group differences, we employed Linear Discriminant Analysis Effect Size (LEfSe) analysis. By assessing the effect size of these differential species through Linear Discriminant Analysis (LDA), the biomarkers significantly enriched in each group were identified. Distance-based redundancy analysis (db-RDA) based on the Bray–Curtis distance algorithm was performed to evaluate the relationship between soil environmental factors and the microbial community.

2.5. Statistical Analysis

A one-way ANOVA (SPSS 26.0, IBM SPSS Statistics Inc., Chicago, IL, USA) with a post hoc Duncan's test was used to analyze the differences between the treatments ($p < 0.05$). A multivariate ANOVA (SPSS 26.0) was employed to examine the effects of treatment groups and cycle numbers on different nitrogen contents under FTCs. Correlation analysis was performed using R (v4.5.1, R Foundation for Statistical Computing, Vienna, Austria) and SPSS 26.0. The Partial Least Squares Structural Equation Modeling (PLS-SEM) analysis was performed using the plspm package (version 0.4.9) in R software. Figures were plotted using Origin 2022pro (OriginLab Corp., Northampton, MA, USA) and R 4.5.1.

3. Results

3.1. Changes in Soil Characteristics

As shown in Figure S1a, freeze-thaw cycles (FTCs) significantly exacerbated soil moisture loss. Soil amended with PBC and UBC enhanced water retention ($p < 0.05$) (Figure 1a). Compared to C0, the FTS group exhibited a 36.57% decrease in soil moisture by C20, while the CTS group showed a reduction of only 11.94%. Relative to FTS, the declines in soil moisture under S + PBC and S + UBC treatments were reduced by 4.99% and 4.68%, respectively. FTCs also influenced the dynamics of soil pH, and the pH changes in the biochar and its fraction treatment group remained relatively stable (Figure S1b). At C20, the pH in CTS decreased by 2.06% compared to the initial value, while that in FTS increased by 2.22%. During the FTCs process, the application of biochar and its fractions significantly improved the pH ($p < 0.05$) and stability of the soil (Figure 1b). Additionally, PBC and DBC markedly raised soil EC during FTCs, while UBC initially decreased soil EC ($p < 0.05$) (Figure 1c). All groups displayed an initial rise followed by a decline in EC (Figure S1c). A single freeze-thaw event caused a pronounced increase, which was most notable in FTS at 11.74%.

Biochar and its fractions significantly improved soil AK during the FTCs process ($p < 0.05$) (Figure 1e), with average improvements ranging from 20.97% to 45.45% compared to FTS, following the order: PBC > DBC > UBC. The soil AK content increased in each group during the early stage (C1–C5) and decreased during the later stage (C10–C20), as shown in Figure S1e. A similar trend was observed in the soil AP content (Figure S1d). While PBC induced the greatest AP enhancement (13.27%) before FTCs (C0), a single freeze-thaw

event temporarily reduced inter-group differences, which reemerged significantly in later stages (Figure 1d).

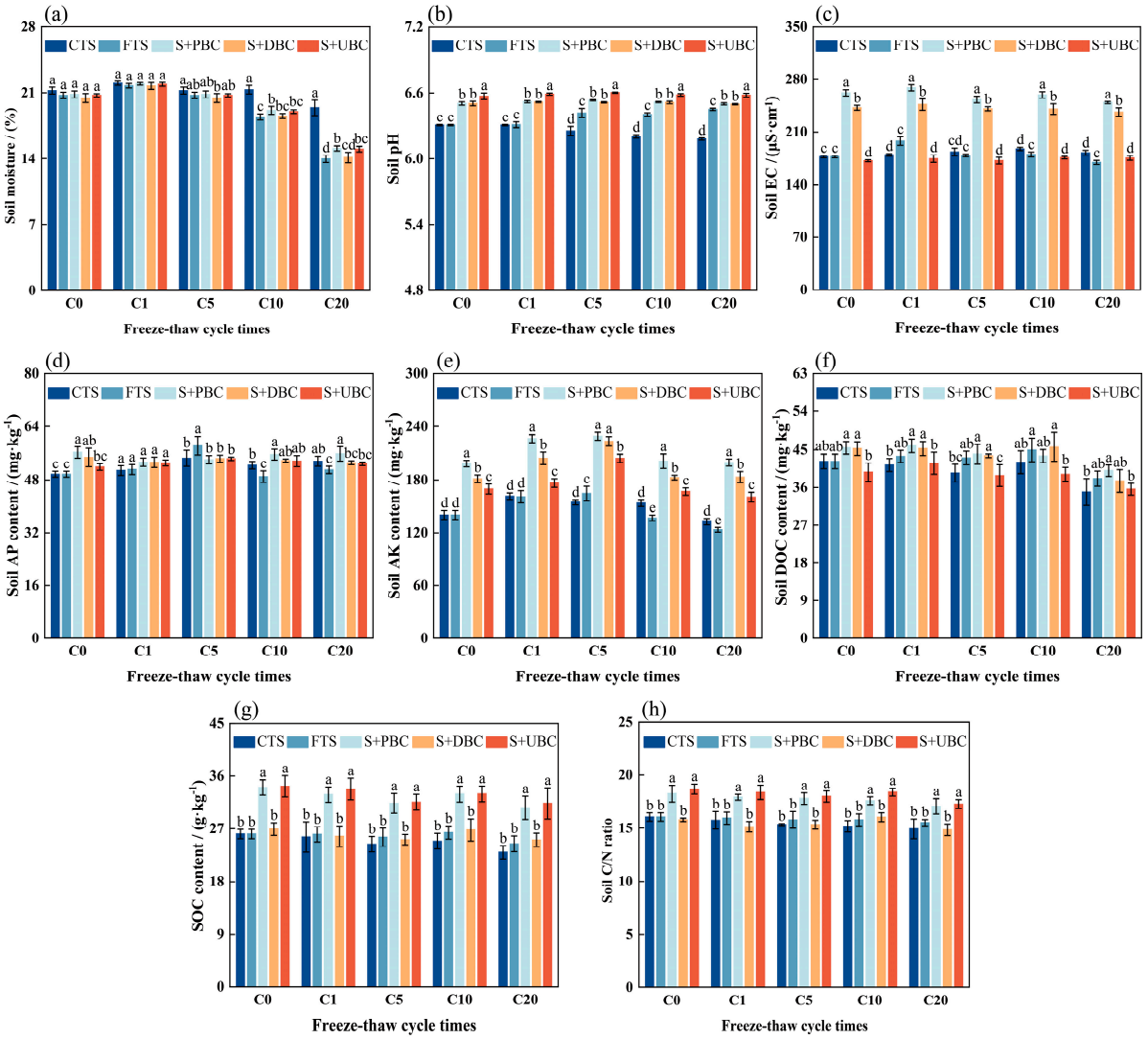

Figure 1. Variation characteristics of soil physicochemical properties. (**a**) soil moisture content, (**b**) pH, (**c**) electrical conductivity (EC), (**d**) available phosphorus (AP) content, (**e**) rapidly-available potassium (AK) content, (**f**) dissolved organic carbon (DOC) content, (**g**) soil total organic carbon (SOC) content, and (**h**) C/N ratio. Different letters indicate significant differences between groups ($p < 0.05$).

The SOC and DOC contents declined fluctuantly during incubation, as shown in Figures S1f,g and 1f,g. PBC and UBC significantly increased SOC ($p < 0.05$), yet also slightly enhanced its loss under FTCs. Furthermore, FTCs decreased the SOC change rate. At C20, the SOC content of CTS, S + PBC, and S + UBC decreased by 11.96%, 10.21%, and 8.46%, respectively; FTS and DBC decreased by 6.44% and 6.87%, respectively. Regarding DOC content, it was significantly higher in both S + PBC and S + DBC at C0 but lower in UBC ($p < 0.05$). As cycling progressed, the DOC difference between FTS and S + DBC gradually diminished. Moreover, FTCs also reduced the DOC change rate, with the greatest reduction (17.31%) in CTS at C20. Additionally, FTCs did not significantly alter the soil carbon-to-nitrogen ratio (C/N) (Figure S1h). PBC and DBC effectively increased the soil C/N ratio during the FTC process (Figure 1h), with a 9.93–16.40% improvement compared to FTS.

3.2. Changes in Soil Nitrogen

As shown in Figure 2a, biochar and its fractions significantly reduced the NH_4^+-N content during the FTC process ($p < 0.05$). S + PBC had the lowest NH_4^+-N content, while there was no obvious difference between S + DBC and S + UBC. NH_4^+-N decreased over time (Figure S2a), with FTCs slowing its consumption. Compared to C0, CTS decreased by 30.43%, contrasting with only 8.14% in FTS, while S + PBC, S + DBC, and S + UBC declined by 6.21%, 8.03%, and 12.50%, respectively. Figure S2b showed that the NO_3^--N content increased with the cycle times, and FTCs reduced the increment in NO_3^--N. Compared to FTS, PBC and UBC led to significant reductions ($p < 0.05$), whereas DBC showed no significant difference (Figure 2b). The highest NO_3^--N content occurred at C20, increasing by 12.67 to 4.9 mg/kg across groups relative to C0. Overall, the inorganic N content exhibited a fluctuating but increasing trend (Figure S2c). Biochar and its fractions significantly reduced inorganic N compared to FTS ($p < 0.05$) (Figure 2c), with the reduction effectiveness following the order: PBC > UBC > DBC.

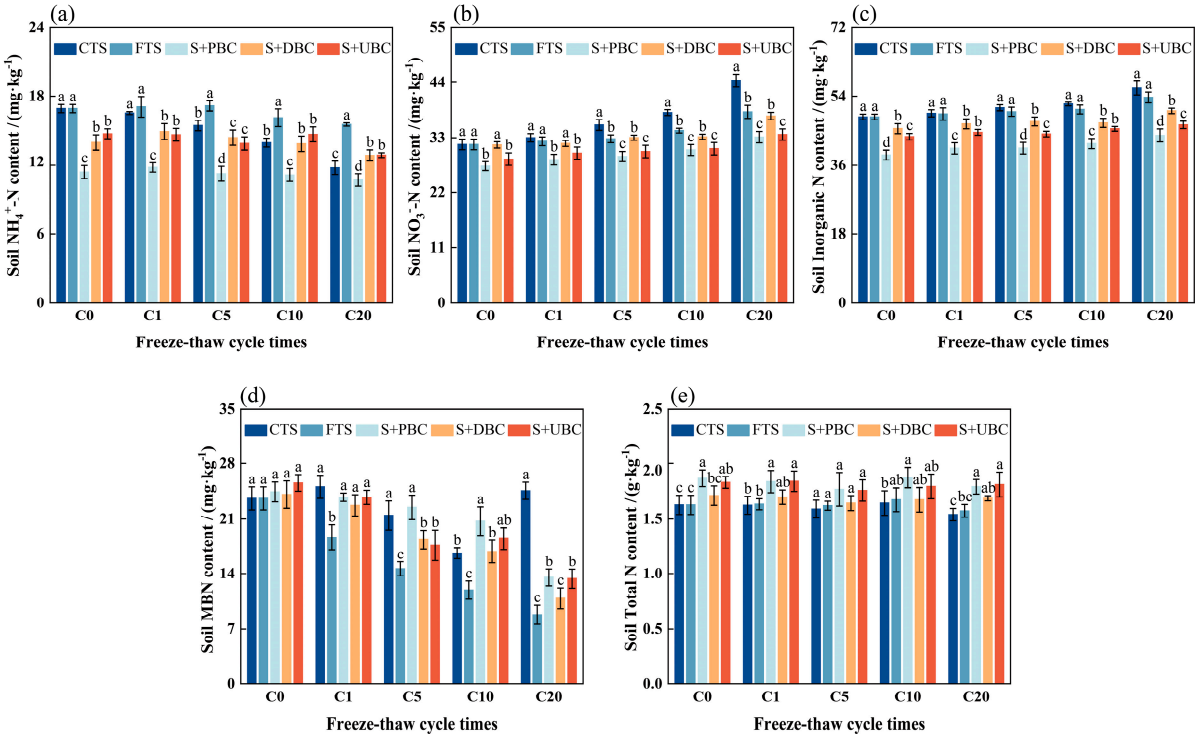

Figure 2. Variation characteristics of soil nitrogen content in different forms. (**a**) ammonium nitrogen (NH_4^+-N) content, (**b**) nitrate nitrogen (NO_3^--N) content, (**c**) inorganic nitrogen (inorganic N) content, (**d**) microbial biomass nitrogen (MBN) content, and (**e**) total nitrogen (total N) content. Different letters indicate significant differences between groups ($p < 0.05$).

FTCs significantly reduced the MBN content, as shown in Figure 2d. Biochar and its fractions effectively mitigated this freeze-thaw-induced damage, with PBC showing the most pronounced protective effect. Although MBN was slightly elevated by all biochar treatments at C0 ($p > 0.05$), it decreased continuously under FTCs from C0 to C20 (Figure S2d). By C20, FTS decreased sharply by 62.74%, while reductions in S + PBC, S + DBC, and S + UBC were 44.67%, 54.89%, and 47.73%, respectively. Meanwhile, the total N content also declined during incubation (Figure S2e). Biochar and its fractions effectively enhanced total N content and reduced total N loss during the FTC process (Figure 2e). At C0, PBC, DBC, and UBC increased total N content by 14.68%, 4.87%, and 12.53%, respectively, compared to FTS. By C20, the total N losses in biochar-treated groups were 0.45–2.32% lower than in FTS.

A multivariate ANOVA was performed on soil nitrogen-related indicators for the treatment groups subjected to FTCs (FTS, S + PBC, S + DBC, S + UBC), examining the individual effects of treatment (T) and FTC number (FTN) as well as their interaction. Table 3 showed that treatment had a significant effect on all soil nitrogen form contents ($p < 0.01$), while FTN had a significant effect on soil nitrogen form contents except total N ($p < 0.01$). Except for MBN, the interaction had no significant effect on the contents of other forms of nitrogen ($p > 0.05$).

Table 3. Multivariate ANOVA results for the effects of treatment (T) and FTC number (FTN).

Factor	NH_4^+-N		NO_3^--N		Inorganic N		MBN		Total N	
	F	***p***	**F**	***p***	**F**	***p***	**F**	***p***	**F**	***p***
FTN	13.46	<0.01	62.01	<0.01	23.35	<0.01	164.19	<0.01	1.13	ns
T	214.30	<0.01	63.64	<0.01	170.33	<0.01	45.73	<0.01	18.83	<0.01
T×TN	1.17	ns	0.69	ns	0.55	ns	3.62	<0.01	0.28	ns

Note: ns indicates no significant difference ($p > 0.05$).

3.3. Changes in Soil Bacterial Communities

The alpha diversity index for each treatment group was calculated based on the 16S sequencing results, as shown in Figure 3a–d. FTCs slightly reduced community diversity and species richness. Biochar and its fraction had little effect on the alpha index under FTC's conditions. Compared with the constant temperature group (CTS), the Shannon index decreased in the groups that underwent FTCs, while the Simpson index increased slightly. FTCs elevated the Ace index and Chao1 index in FTS, S + DBC, and S + UBC, while PBC showed a slight decrease. But these differences were not significant ($p > 0.05$).

Figure 3e shows the relative abundance of microbes at the phylum level. The dominant bacterial phyla in each treatment group were mainly *Actinobacteriota*, *Proteobacteria*, *Chloroflexi*, *Acidobacteriota*, and *Firmicutes*, accounting for more than 80% of the relative abundance. Compared with CTS and FTS, FTCs increased the relative abundance of *Actinobacteriota* and *Proteobacteria*, but decreased the relative abundance of *Chloroflexi* and *Acidobacteriota*. The results of cluster analysis (Figure S1) show that the microbial composition in CTS was more similar to those in S + PBC, S + UBC, and S + DBC, and obviously different from those in FTS.

Beta diversity of the microbial community structure across treatment groups was analyzed using Principal Coordinates Analysis (PCoA) based on the Euclidean distance dissimilarity (Figure 3f). ANOSIM test results indicated significant differences in community structure among the treatment groups ($R^2 = 0.21778$, $p = 0.041$). Principal coordinates 1 and 2 (PC1 and PC2) together explained 78.05% of the total variation. CTS showed clear separation from FTS and DBC along the PC1 axis, while exhibiting overlap with PBC and UBC. Furthermore, the application of biochar and its fractions increased the dispersion of bacterial communities after FTCs. To further identify characteristic species features across treatments, we conducted an LEfSe analysis utilizing Linear Discriminant Analysis (LDA) (LDA > 2, $p < 0.05$) to pinpoint group-specific biomarkers. The results are shown in Figure 3g,h. The biomarkers with the highest scores in each group were as follows: *Ellin6067* in CTS, *Halobacillus* in FTS, *SAR202_clade* in PBC, *Rhodococcus* in DBC, and *Azospirillaceae* in UBC.

Distance-based redundancy analysis (db-RDA) based on the Bray-Curtis distance algorithm revealed the relationship between soil environmental factors and the microbial community. To mitigate the influence of multicollinearity among factors, environmental variables with a variance inflation factor (VIF) < 10 were selected for db-RDA through VIF analysis. As shown in Figure 4, CAP1 and CAP2 together explained 41.24% of the

total variance. Among the environmental factors, total N and NO_3^--N showed significant correlations with community structure ($p < 0.05$). Among the top five most abundant bacterial phyla, *Actinobacteriota* was most affected by SOC, *Acidobacteriota* was positively correlated with soil moisture, and *Chloroflexi* was strongly correlated with AP.

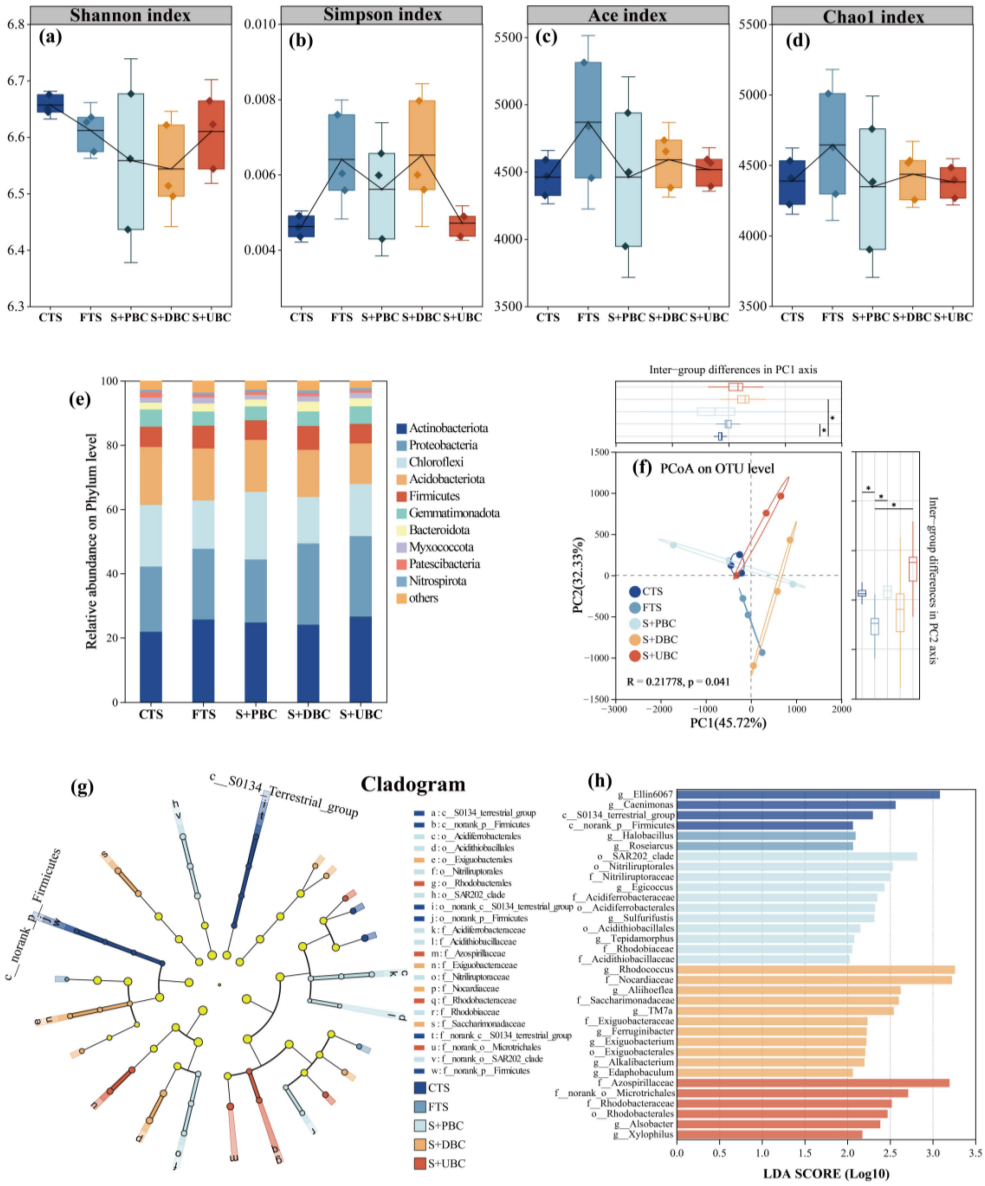

Figure 3. (**a**–**d**) Box plots of alpha diversity indices for each treatment group, where (**a**) Shannon index, (**b**) Simpson index, (**c**) Ace index, (**d**) Chao1 index. (**e**) Plot of microbial relative abundance across treatment groups at the phylum level. (**f**) PCoA results for microbial community distribution (beta diversity), the different information represented by the PC1 axis and PC2 axis were labeled on the boxplots at the top and right side of the figure, respectively. * $p < 0.05$. (**g**,**h**) Biomarkers identified by LEfSe analysis between groups, where (**g**) Cladogram illustrated the distribution of intergroup differential biomarkers from phylum to genus. Concentric rings from inner to outer layers represent different taxonomic levels, with biomarkers significantly enriched in specific groups displayed in corresponding colors. The lowercase letters in the figure represent biomarkers from the phylum to the family level. (**h**) Linear discriminant analysis (LDA) score plot, where bar length reflected the effects of biomarkers across different groups.

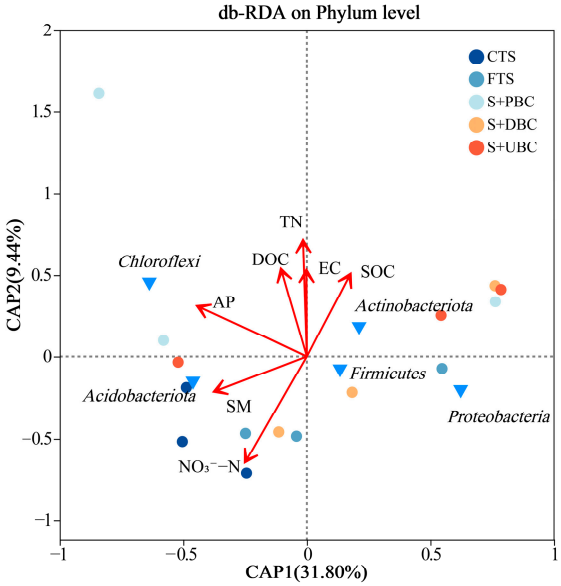

Figure 4. Redundancy analysis results of the association between microorganisms and environmental factors. Red arrows denote different environmental factors, while blue triangles represent dominant microorganisms (at the phylum level).

Partial least squares structural equation modeling (PLS-SEM) was employed to investigate how freeze-thaw cycles (FTCs) and the application of biochar or its fractions (BC) influence advantageous communities and microbial diversity by mediating soil physicochemical and nutrient characteristics. The results are shown in Figure 5. Soil physicochemical properties were regulated by BC (path coefficient = 0.2045, $p < 0.001$) and FTCs (path coefficient = 0.8525, $p < 0.001$). Soil nutrient characteristics were significantly influenced by BC (path coefficient = 0.8393, $p < 0.001$). Microbial diversity was influenced by advantageous communities (path coefficient = 0.6778, $p < 0.001$) and physicochemical characteristics (path coefficient = 0.4392, $p < 0.05$). BC and FTC indirectly influenced microbial diversity by regulating physicochemical characteristics.

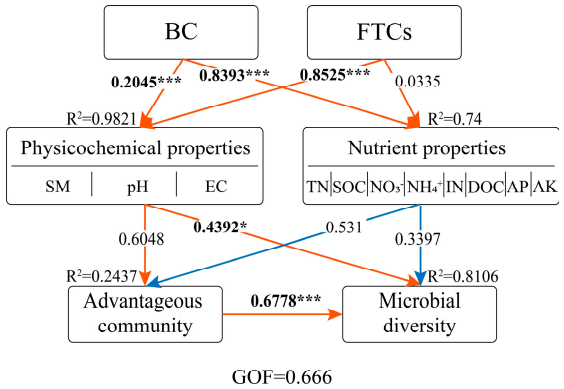

Figure 5. Partial least squares structural equation modeling (PLS-SEM) explains how biochar or its fractions and FTCs exert indirect effects on dominant species and community diversity by influencing soil physical properties and nutrient properties. R^2 value represents the degree of variance explained. The red and blue paths represent positive effects and negative effects, respectively. * $p < 0.05$; *** $p < 0.001$.

4. Discussion

4.1. The Effects of Biochar Fractions and Freeze-Thaw Cycles on Soil Characteristics

During the freeze-thaw cycles (FTCs) process, soil moisture undergoes frequent solid-liquid conversion. These phase changes of moisture cause the agglomerates to break and alter the migration of water and salt, thereby aggravating water dispersion. The moisture content trends in the S + PBC and S + UBC groups were generally consistent (Figure S1a), indicating that the improvement of soil water retention capacity by biochar (PBC) was mainly attributed to the undissolved biochar fractions (UBC). This was due to biochar particles reducing moisture loss by modifying soil pore structure [40]. The soil pH in the freeze-thaw control group (FTS) showed a positive correlation with cycle numbers, which was related to the release of alkaline cations and organic anions from soil aggregates [41]. The addition of biochar and its fractions can increase soil pH and effectively reduce the correlation between cycle times and soil pH (Table S1). This result can be attributed to the liming effect of alkaline biochar and its oxygen-containing functional groups, which enhanced soil pH and buffering capacity [42].

FTCs disturb the physical structure of soil, causing changes in soil EC, AP, and AK content [43]. The EC, AP, and AK contents observed in S + PBC and S + DBC treatments were more similar (Figure 1c–e), indicating that the enhancement of these properties is closely related to the dissolved fraction of biochar. Biochar produced at higher pyrolysis temperatures contains a greater proportion of residual inorganic minerals [44]. Therefore, the application of both PBC and DBC significantly increased EC throughout the FTC's process. In contrast, UBC slightly reduced EC in the early stage, likely due to enhanced adsorption of ions from the soil solution after ash removal. Furthermore, high-temperature conditions promote the retention and accumulation of total phosphorus and total potassium in biochar [45]. The phosphorus and potassium in biochar are primarily present in the ash as phosphates and potassium salts. This also explains the reason why PBC and DBC enhance soil AK and AP. Water washing treatment removed most of the ash from biochar, which greatly diminished the ability of UBC to supply AP. Nevertheless, the exchangeable potassium present in biochar allows UBC to maintain a stable supply of AK to the soil [46].

FTCs reduced the consumption of the original SOC and DOC in the soil. The inhibitory effect of FTCs on microbial activity slowed down the mineralization rate of SOC [47]. Therefore, compared to CTS, FTS showed a reduction in the consumption of SOC. Biochar produced at high temperatures exhibits higher levels of recalcitrant carbon [48]. Consequently, the significant increase in SOC content observed under S + PBC and S + UBC treatments indicated that biochar's contribution to soil carbon pool enhancement primarily relies on recalcitrant carbon supplied by undissolved fractions. However, the negative correlation coefficients between SOC and cycle times were higher in the S + PBC and S + UBC groups (Table S1). This can be attributed to the fragmentation of FTCs that accelerates the aging of biochar and increases the consumption of SOC by soil microorganisms [49]. Additionally, biochar can accelerate microbial mineralization of organic carbon through a priming effect [50]. Meanwhile, FTCs led to an initial increase followed by a subsequent decrease in soil DOC, consistent with the findings observed by Zhang et al. [51]. The early stage of FTCs raised soil DOC levels by disrupting aggregates and lysing microbial cells [52], thereby reducing differences between treatments participating in FTCs. After adapting to FTCs, the surviving microorganisms rapidly consumed DOC. Therefore, the DOC content of each treatment group participating in FTCs decreased significantly in the later incubation period. The addition of biochar and its fractions enhanced the correlation between soil DOC and cycle times, with S + PBC having the highest correlation coefficient (Table S1). Previous studies have demonstrated that FTCs promote the fragmentation of

biochar and release dissolved carbon [53], which leads to increased microbial utilization and consumption.

4.2. The Effect of Biochar Fractions and Freeze-Thaw on Soil Nitrogen

A comparison between the constant temperature group (CTS) and the freeze-thaw control group (FTS) can help us understand the impact of FTCs on soil nitrogen. In general, FTCs regulate soil nitrogen content mainly through form restructuring rather than total loss (Figure 2a–e). FTCs had a significant negative effect on soil NH_4^+-N consumption, NO_3^--N accumulation, and MBN ($p < 0.05$). However, FTCs had no significant effect on soil inorganic N and total N ($p > 0.05$).

FTCs caused the NH_4^+-N contents to increase initially and subsequently decrease (Figure S2a), which is consistent with the findings of previous research [54]. This trend can be attributed to the FTCs disrupting soil physical structure, releasing organic matter, and influencing ammonification and nitrogen mineralization processes. Low temperatures also inhibited microbial assimilation of NH_4^+-N. Compared to CTS, the lower NO_3^--N content in FTS (Figure S2b) can be attributed to the inhibition of nitrification at low temperature [55]. The dynamic variation differences between NH_4^+-N and NO_3^--N led to changes in the composition of inorganic N, but the impact on inorganic N content was not significant under FTCs. This may be related to the mineralization-fixation equilibrium background of the constant temperature group (CTS). In the CTS group, the cycle numbers showed a significant negative correlation with MBN. This result also corroborates previous studies indicating the stress effect of FTCs on microorganisms [56]. The reduction in MBN resulted from both the direct physical damage to cells caused by ice crystals and the indirect effects of disturbance to the soil environment. FTCs had little effect on the total N content, which is consistent with the findings of previous research [57]. Their study indicated that FTCs mainly alter the distribution of soil nitrogen forms, without significantly affecting the total soil nitrogen pool.

Overall, the trends in soil nitrogen contents in the biochar and its fraction treatment groups during the FTCs process were basically consistent with FTS (Figure S2a–e). The results in Table 3 showed that there was no significant interaction between the FTC numbers and treatments on the regulation of NH_4^+-N, NO_3^--N, inorganic N, and total N contents. This suggested that the regulatory differences of these soil nitrogen forms caused by biochar and its fraction were stable under freeze-thaw disturbance. Different fractions of biochar exhibited distinct mechanisms for regulating nitrogen forms. Similar to the changes in SOC, PBC and UBC considerably increased the total N content, while DBC only slightly increased it. This result showed that the increment of total N by biochar was mainly achieved through the exogenous nitrogen input of the undissolved biochar fraction. As shown in Figure S2a,b, during the entire FTC process, PBC and UBC significantly reduced the content of NH_4^+-N and NO_3^--N. DBC only significantly reduced the content of NH_4^+-N. Therefore, the reduction in inorganic nitrogen followed the pattern PBC > UBC > DBC (Figure S2c). Beyond adsorption, the significant negative correlation between NO_3^--N, inorganic N content, and C/N ratio (Figure S4) provided evidence that biochar can reduce soil inorganic nitrogen content by enhancing microbial assimilation, a mechanism that is supported by previous studies [58]. In addition to adsorption and enhanced microbial assimilation, the observed reduction in NO_3^--N may also be partially attributable to potential stimulation of denitrification. Studies indicate that biochar's ability to raise pH in nearby areas and enhance electron transfer may reduce nitrate nitrogen by promoting denitrification processes [59]. The S + DBC treatment still showed a reduction in NH_4^+-N in the absence of carbon frame adsorption. Correlation analysis indicates that NH_4^+-N content exhibits a significant negative correlation with soil EC (Figure S4).

The increase in EC can enhance charge interactions, facilitating the migration of bound NH_4^+-N into the soil solution [60], thereby increasing its bioavailability and consumption. Therefore, the reduction in soil NH_4^+-N by biochar was derived from the combined effects of its two fractions, while the reduction in nitrate nitrogen primarily derives from the undissolved fraction.

Simultaneously, biochar and its fractions effectively mitigated the negative impact of FTCs on MBN. The variation trends of MBN in S + PBC, S + DBC, and S + UBC further demonstrated the crucial role of microbial assimilation in nitrogen transformation. During the later stages of FTCs, the regulatory capacity of biochar and its fraction on MBN was weakened (Figure S2). Similarly, a significant interaction was observed between the FTC numbers and treatments on the MBN (Table 3). Correlation analysis (Figure S4) revealed a significant positive relationship between MBN and both SOC and soil moisture in the groups subjected to FTCs. This can be attributed to the physical structure of biochar providing shelter for microorganisms, while its nutrient input supports microbial activity [61]. These results showed that under long-term FTCs, biochar mitigated the stress of FTCs on microbial nitrogen by enhancing water retention and organic carbon pools through its undissolved fraction, which was consistent with our hypothesis.

4.3. Effects of Biochar Fractions and Freeze-Thaw Cycles on Soil Microorganisms

In this study, no significant differences were observed in the alpha diversity of microbial communities among the groups. A meta-analysis [62] also indicated that microbial alpha diversity does not decrease significantly under FTCs, except in field and wetland ecosystems. Changes in dominant bacterial phyla under FTCs (Figure 3e) reflected microbial community responses to freeze-thaw stress. Clustering results (Figure S3) and PCoA analysis (Figure 3f) further indicated that biochar and its fractions modulated freeze-thaw stress, shifting community structure closer to that observed under constant temperature control (CTS). Redundancy analysis results (Figure 4) suggested that TN and NO_3^--N were the major drivers regulating microbial composition. Biochar can modulate microbial composition by influencing nitrogen pools, with the undissolved fraction (UBC) playing a primary role through altering soil total N and NO_3^--N. These results supported the first hypothesis, that biochar fractions exert distinct regulatory effects on microbial communities. Partial least squares structural equation modeling (PLS-SEM) revealed the indirect regulatory mechanisms by BC (biochar or its fraction) and FTCs on microbial diversity (Figure 5). The model reveals that soil physicochemical characteristics were co-regulated by both FTCs and BC, with FTCs exerting a stronger influence. In contrast, soil nutrient properties were significantly affected only by BC. Microbial community diversity was positively influenced by dominant species and soil physicochemical properties but negatively affected by soil nutrient properties. Among these factors, dominant species and soil physicochemical properties had more substantial effects. These findings suggested that under FTC conditions, improving soil physicochemical properties may be more effective for maintaining microbial community diversity.

Besides, analyzing biomarkers in LEfSe results (Figure 3g,h) can help in understanding the effects of each treatment group on microbial communities. In CTS, the significant enrichment of *Ellin6067* (a nitrifying bacterium) [63] explained the highest NO_3^--N content observed in this group, while the enrichment of *Caenimonas* may indicate soil nutrient deficiency [64]. The biomarkers with higher scores (LDA > 2.5) in the treatment group for biochar and its fractions primarily represent microorganisms involved in the degradation of complex organic matter, such as *Nitriliruptoraceae* and *SAR202_clade* (S + PBC) [65,66], *Rhodococcus* and *Nocardiaceae* (S + DBC) [67,68], and *Microtrichales* (S + UBC) [69]. This indicates that under FTC conditions, biochar and its components were still able to enrich

functional microorganisms through the input of exogenous organic carbon, thereby promoting soil carbon and nitrogen cycling. Furthermore, the enrichment of *Microtrichales* within UBC indicated a promotion of aggregate stability. However, it is noteworthy that a higher concentration of salt-tolerant bacteria, such as *Egicoccus*, *Rhodococcus*, and *Exiguobacterium*, was observed in the biomarkers of PBC and DBC [70,71]. This result alarms us that the application of high-salinity biochar may pose risks of salinity stress.

5. Conclusions

This study demonstrated that biochar fractions exert differing effects on the soil environment under freeze-thaw conditions. The undissolved biochar fraction (UBC) primarily reduced soil moisture loss and enhanced total nutrient pools (SOC, total N), while the dissolved biochar fraction (DBC) mainly increased electrical conductivity and readily available nutrients (AP, AK, DOC) during the FTCs process. In terms of nitrogen form regulation, biochar and its fractions maintained stable regulatory effects on NH_4^+-N, NO_3^--N, inorganic N, and total N during the FTCs process. The reduction in NH_4^+-N resulted from the combined action of both fractions, while the reduction in NO_3^--N was primarily driven by the undissolved biochar fraction. By enhancing water retention capacity and carbon supply, PBC and UBC promoted the retention of MBN during FTC's progress. Under the FTC's conditions, biochar and its fractions enriched different biomarkers but did not directly affect community diversity. Partial least squares structural equation modeling (PLS-SEM) further revealed that changes in soil physicochemical properties exerted a stronger influence on microbial community structure than nutrient properties. These findings demonstrate that the undissolved fraction of biochar is the primary mechanism supporting biochar's mitigation of freeze-thaw stress in soil. Our findings provided new insights into the regulation of cold-region soil environments by biochar at the fraction scale.

Supplementary Materials: The following supporting information can be downloaded at: https://www.mdpi.com/article/10.3390/agronomy15102437/s1, S1: DNA extraction, 16S rRNA gene amplification, and sequencing methods; Table S1: Correlation coefficient between the cycle numbers and soil physicochemical factors; Figure S1: The changes in characteristics of soil physicochemical properties. (a) soil moisture content, (b) pH, (c) electrical conductivity (EC), (d) available phosphorus (AP) content, (e) rapidly-available potassium (AK) content, (f) dissolved organic carbon (DOC) content, (g) soil total organic carbon (SOC) content, and (h) C/N ratio; Figure S2: The changes in nitrogen form content in the soil across treatment groups. (a) ammonium nitrogen (NH_4^+-N) content, (b) nitrate nitrogen (NO_3^--N) content, (c) inorganic nitrogen (inorganic N) content, (d) microbial biomass nitrogen (MBN) content, and (e) total nitrogen (total N) content; Figure S3: Clustering heatmap of community abundance at the phylum level across treatment groups; Figure S4: Heatmap of correlation between physicochemical factors across treatment groups under FTCs condition.

Author Contributions: X.G.: conceptualization, methodology, investigation, data curation, formal analysis, writing—original draft, visualization. Y.W.: investigation, data curation, writing—review and editing. M.L.: conceptualization, writing—review and editing, funding acquisition. J.Y.: methodology, writing—review and editing. S.H.: supervision, conceptualization, writing—review & editing. All authors have read and agreed to the published version of the manuscript.

Funding: This research was funded by the Fundamental Research Funds for the Central Universities (2572022BA09); Natural Science Foundation of Heilongjiang Province of China (LH2023D003).

Data Availability Statement: The data presented in this study are available upon request from the corresponding author. The data are not publicly available due to privacy requirements.

Acknowledgments: The authors gratefully acknowledge funding supported by the Fundamental Research Funds for the Central Universities (2572022BA09) and the Natural Science Foundation of Heilongjiang Province of China (LH2023D003). During the preparation of this manuscript, the

authors used DeepL and DeepSeek-V3 for the purposes of translation and language improvement. The authors have reviewed and edited the output and take full responsibility for the content of this publication.

Conflicts of Interest: The authors declare no conflicts of interest.

Abbreviations

The following abbreviations are used in this manuscript:

FTCs	Freeze-thaw cycles
FTN	Freeze-thaw cycle number
N	Nitrogen
PBC	Pristine biochar
DBC	Dissolved fraction of biochar
UBC	Undissolved fraction of biochar
CTS	Constant temperature control soil
FTS	Freeze-thaw control soil
S + PBC	Soil with PBC treatment
S + DBC	Soil with DBC treatment
S + UBC	Soil with UBC treatment
EC	Electrical conductivity
NH_4^+-N	Ammonium nitrogen
NO_3^--N	Nitrate nitrogen
MBN	Microbial biomass nitrogen
SOC	Soil total organic carbon
AP	Available phosphorus
AK	Rapidly-available potassium
DOC	Dissolved organic carbon

References

1. Harrison, J.L.; Sanders-DeMott, R.; Reinmann, A.B.; Sorensen, P.O.; Phillips, N.G.; Templer, P.H. Growing-season warming and winter soil freeze/thaw cycles increase transpiration in a northern hardwood forest. *Ecology* **2020**, *101*, e03173. [CrossRef] [PubMed]
2. Kreyling, J.; Beierkuhnlein, C.; Pritsch, K.; Schloter, M.; Jentsch, A. Recurrent soil freeze–thaw cycles enhance grassland productivity. *New Phytol.* **2007**, *177*, 938–945. [CrossRef] [PubMed]
3. Wang, J.; Qian, R.; Li, J.; Wei, F.; Ma, Z.; Gao, S.; Sun, X.; Zhang, P.; Cai, T.; Zhao, X.; et al. Nitrogen reduction enhances crop productivity, decreases soil nitrogen loss and optimize its balance in wheat-maize cropping area of the Loess Plateau, China. *Eur. J. Agron.* **2024**, *161*, 127352. [CrossRef]
4. Shibata, H. Impact of winter climate change on nitrogen biogeochemistry in forest ecosystems: A synthesis from Japanese case studies. *Ecol. Indic.* **2016**, *65*, 4–9. [CrossRef]
5. Urakawa, R.; Shibata, H.; Kuroiwa, M.; Inagaki, Y.; Tateno, R.; Hishi, T.; Fukuzawa, K.; Hirai, K.; Toda, H.; Oyanagi, N.; et al. Effects of freeze–thaw cycles resulting from winter climate change on soil nitrogen cycling in ten temperate forest ecosystems throughout the Japanese archipelago. *Soil Biol. Biochem.* **2014**, *74*, 82–94. [CrossRef]
6. Joseph, G.; Henry, H.A.L. Soil nitrogen leaching losses in response to freeze–thaw cycles and pulsed warming in a temperate old field. *Soil Biol. Biochem.* **2008**, *40*, 1947–1953. [CrossRef]
7. Kamali, M.; Sweygers, N.; Al-Salem, S.; Appels, L.; Aminabhavi, T.M.; Dewil, R. Biochar for soil applications-sustainability aspects, challenges and future prospects. *Chem. Eng. J.* **2022**, *428*, 131189. [CrossRef]
8. Brtnicky, M.; Datta, R.; Holatko, J.; Bielska, L.; Gusiatin, Z.M.; Kucerik, J.; Hammerschmiedt, T.; Danish, S.; Radziemska, M.; Mravcova, L.; et al. A critical review of the possible adverse effects of biochar in the soil environment. *Sci. Total Environ.* **2021**, *796*, 148756. [CrossRef]
9. Sun, Y.; Xiong, X.; He, M.; Xu, Z.; Hou, D.; Zhang, W.; Ok, Y.S.; Rinklebe, J.; Wang, L.; Tsang, D.C.W. Roles of biochar-derived dissolved organic matter in soil amendment and environmental remediation: A critical review. *Chem. Eng. J.* **2021**, *424*, 130387. [CrossRef]
10. Graber, E.R.; Tsechansky, L.; Lew, B.; Cohen, E. Reducing capacity of water extracts of biochars and their solubilization of soilMn andFe. *Eur. J. Soil Sci.* **2013**, *65*, 162–172. [CrossRef]

11. Smith, C.R.; Buzan, E.M.; Lee, J.W. Potential Impact of Biochar Water-Extractable Substances on Environmental Sustainability. *ACS Sustain. Chem. Eng.* **2012**, *1*, 118–126. [CrossRef]
12. Locaspi, A.; Debiagi, P.; Pelucchi, M.; Hasse, C.; Faravelli, T. A Predictive Physico-chemical Model of Biochar Oxidation. *Energy Fuels* **2021**, *35*, 14894–14912. [CrossRef]
13. Qu, X.; Fu, H.; Mao, J.; Ran, Y.; Zhang, D.; Zhu, D. Chemical and structural properties of dissolved black carbon released from biochars. *Carbon* **2016**, *96*, 759–767. [CrossRef]
14. Yang, F.; Chen, Y.; Huang, Y.; Cao, X.; Zhao, L.; Qiu, H.; Xu, X. New insights into the underlying influence of bentonite on Pb immobilization by undissolvable and dissolvable fractions of biochar. *Sci. Total Environ.* **2021**, *775*, 145824. [CrossRef] [PubMed]
15. Shi, R.-Y.; Ni, N.; Wang, R.-H.; Nkoh, J.N.; Pan, X.-Y.; Dong, G.; Xu, R.-K.; Cui, X.-M.; Li, J.-Y. Dissolved biochar fractions and solid biochar particles inhibit soil acidification induced by nitrification through different mechanisms. *Sci. Total Environ.* **2023**, *874*, 162464. [CrossRef] [PubMed]
16. Huang, X.; Zhang, C.; Zhu, S.; Chen, D.; Ho, S.-H. Effects of Biochar on Microalgal Growth: Difference between Dissolved and Undissolved Fractions. *ACS Sustain. Chem. Eng.* **2020**, *8*, 9156–9164. [CrossRef]
17. Han, L.; Liu, B.; Luo, Y.; Chen, L.; Ma, C.; Xu, C.; Sun, K.; Xing, B. Quantifying the negative effects of dissolved organic carbon of maize straw-derived biochar on its carbon sequestration potential in a paddy soil. *Soil Biol. Biochem.* **2024**, *196*, 109500. [CrossRef]
18. Lehmann, J.; Rillig, M.C.; Thies, J.; Masiello, C.A.; Hockaday, W.C.; Crowley, D. Biochar effects on soil biota–A review. *Soil Biol. Biochem.* **2011**, *43*, 1812–1836. [CrossRef]
19. Zhang, C.; Huang, X.; Zhang, X.; Wan, L.; Wang, Z. Effects of biochar application on soil nitrogen and phosphorous leaching loss and oil peony growth. *Agric. Water Manag.* **2021**, *255*, 107022. [CrossRef]
20. Hailegnaw, N.S.; Mercl, F.; Pračke, K.; Száková, J.; Tlustoš, P. High temperature-produced biochar can be efficient in nitrate loss prevention and carbon sequestration. *Geoderma* **2019**, *338*, 48–55. [CrossRef]
21. Tan, Z.; Ye, Z.; Zhang, L.; Huang, Q. Application of the 15N tracer method to study the effect of pyrolysis temperature and atmosphere on the distribution of biochar nitrogen in the biomass–biochar-plant system. *Sci. Total Environ.* **2018**, *622–623*, 79–87. [CrossRef]
22. Zheng, H.; Wang, Z.; Deng, X.; Herbert, S.; Xing, B. Impacts of adding biochar on nitrogen retention and bioavailability in agricultural soil. *Geoderma* **2013**, *206*, 32–39. [CrossRef]
23. Liu, L.; Wang, Y.; Yan, X.; Li, J.; Jiao, N.; Hu, S. Biochar amendments increase the yield advantage of legume-based intercropping systems over monoculture. *Agric. Ecosyst. Environ.* **2017**, *237*, 16–23. [CrossRef]
24. Wang, Z.; Zheng, H.; Luo, Y.; Deng, X.; Herbert, S.; Xing, B. Characterization and influence of biochars on nitrous oxide emission from agricultural soil. *Environ. Pollut.* **2013**, *174*, 289–296. [CrossRef] [PubMed]
25. Zhou, Y.; Berruti, F.; Greenhalf, C.; Tian, X.; Henry, H.A.L. Increased retention of soil nitrogen over winter by biochar application: Implications of biochar pyrolysis temperature for plant nitrogen availability. *Agric. Ecosyst. Environ.* **2017**, *236*, 61–68. [CrossRef]
26. Li, Q.; Fu, Q.; Li, T.; Liu, D.; Hou, R.; Li, M.; Gao, Y. Biochar impacts on the soil environment of soybean root systems. *Sci. Total Environ.* **2022**, *821*, 153421. [CrossRef]
27. Yang, X.; Hou, R.; Fu, Q.; Li, T.; Wang, J.; Su, Z.; Shen, W.; Zhou, W.; Wang, Y. Effect of freeze-thaw cycles and biochar coupling on the soil water-soil environment, nitrogen adsorption and N2O emissions in seasonally frozen regions. *Sci. Total Environ.* **2023**, *893*, 164845. [CrossRef]
28. Yang, Z.; She, R.; Hu, L.; Yu, Y.; Yao, H. Effects of biochar addition on nitrous oxide emission during soil freeze–thaw cycles. *Front. Microbiol.* **2022**, *13*, 1033210. [CrossRef]
29. Shi, G.; Hou, R.; Li, T.; Fu, Q.; Wang, J.; Zhou, W.; Su, Z.; Shen, W.; Wang, Y. Effects of biochar and freeze–thaw cycles on the bacterial community and multifunctionality in a cold black soil area. *J. Environ. Manag.* **2023**, *342*, 118302. [CrossRef]
30. Han, Z.; Deng, M.; Yuan, A.; Wang, J.; Li, H.; Ma, J. Vertical variation of a black soil's properties in response to freeze-thaw cycles and its links to shift of microbial community structure. *Sci. Total Environ.* **2018**, *625*, 106–113. [CrossRef]
31. Zhao, Z.; Zhang, H.; Duan, Y.; Sun, L.; Pang, X.; Wang, X.; Tang, X. Varieties of P fractions in biochar-amended reconstructed soils as impacted by freeze-thaw interference. *J. Environ. Manag.* **2024**, *366*, 121839. [CrossRef]
32. Zhao, P.; Gao, X.; Liu, D.; Sun, Y.; Li, M.; Han, S. Effect of different biochar additions on the change of carbon nitrogen content and bacterial community in meadow soils. *Environ. Pollut. Bioavailab.* **2023**, *35*, 2268272. [CrossRef]
33. *NY/T 1848-2010*; Method for Determination of Ammonium Nitrogen, Available Phosphorus and Rapidly-Available Potassium in Neutrality or Calcareous Soil Universal Extract-Colorimetric Method. China Agriculture Press: Beijing, China, 2010.
34. Lin, Q.; Wu, Y.; Liu, H. Modification of fumigation extraction method for measuring soil microbial biomass carbon. *Chin. J. Ecol.* **1999**, *18*, 63–66. [CrossRef]
35. *HJ 615-2011*; Soil-Determination of Organic Carbon-Potassium Dichromate Oxidation Spectrophotometric Method. China Environmental Science Press: Beijing, China, 2011.
36. *GB/T 42485-2023*; Soil Quality—Determination of Nitrate, Nitrite and Ammonium in Soils—Extraction with Potassium Chloride Solution and Determination. Standards Press of China: Beijing, China, 2023.

37. *GB/T 32737-2016*; Determination of Nitrate Nitrogen in Soil—Ultraviolet Spectrophotometry Method. Standards Press of China: Beijing, China, 2016.
38. *GB/T 39228-2020*; Determination of Soil Microbial Biomass—Fumigation-Extraction Method. Standards Press of China: Beijing, China, 2020.
39. Yu, J.; Zhang, X.; Zhang, Z.; Guo, H.; Noborio, K.; Han, S. Effects of bioremediation on soil fertility and microbial communities of degraded grassland soil under dual petroleum contamination and saline-alkali stress. *J. For. Res.* **2025**, *36*, 20. [CrossRef]
40. Fu, Q.; Zhao, H.; Li, T.; Hou, R.; Liu, D.; Ji, Y.; Zhou, Z.; Yang, L. Effects of biochar addition on soil hydraulic properties before and after freezing-thawing. *Catena* **2019**, *176*, 112–124. [CrossRef]
41. Sun, S.; Yu, S.; Du, R.; Wang, Y.; Kang, C. Freeze-thaw effect on adsorption and transport of two sulfonamides in soil: Batch and column studies. *J. Contam. Hydrol.* **2025**, *269*, 104509. [CrossRef]
42. Shi, R.-y.; Hong, Z.-n.; Li, J.-y.; Jiang, J.; Baquy, M.A.-A.; Xu, R.-k.; Qian, W. Mechanisms for Increasing the pH Buffering Capacity of an Acidic Ultisol by Crop Residue-Derived Biochars. *J. Agric. Food Chem.* **2017**, *65*, 8111–8119. [CrossRef]
43. Li, J.; Qi, X.; Wang, F.; Che, Y.; Qu, J.; Sun, Y. Effect of Straw Biochar on Availability of Phosphorus in Black Soil During Freeze-Thaw Period. *J. Soil Sci. Plant Nutr.* **2025**, *25*, 5020–5031. [CrossRef]
44. He, X.; Liu, Z.; Niu, W.; Yang, L.; Zhou, T.; Qin, D.; Niu, Z.; Yuan, Q. Effects of pyrolysis temperature on the physicochemical properties of gas and biochar obtained from pyrolysis of crop residues. *Energy* **2018**, *143*, 746–756. [CrossRef]
45. Tu, P.; Zhang, G.; Wei, G.; Li, J.; Li, Y.; Deng, L.; Yuan, H. Influence of pyrolysis temperature on the physicochemical properties of biochars obtained from herbaceous and woody plants. *Bioresour. Bioprocess.* **2022**, *9*, 131. [CrossRef]
46. Xiu, L.; Gu, W.; Sun, Y.; Wu, D.; Wang, Y.; Zhang, H.; Zhang, W.; Chen, W. The fate and supply capacity of potassium in biochar used in agriculture. *Sci. Total Environ.* **2023**, *902*, 165969. [CrossRef]
47. Matzner, E.; Borken, W. Do freeze-thaw events enhance C and N losses from soils of different ecosystems? A review. *Eur. J. Soil Sci.* **2008**, *59*, 274–284. [CrossRef]
48. Liu, C.-H.; Chu, W.; Li, H.; Boyd, S.A.; Teppen, B.J.; Mao, J.; Lehmann, J.; Zhang, W. Quantification and characterization of dissolved organic carbon from biochars. *Geoderma* **2019**, *335*, 161–169. [CrossRef]
49. Wang, L.; O'Connor, D.; Rinklebe, J.; Ok, Y.S.; Tsang, D.C.W.; Shen, Z.; Hou, D. Biochar Aging: Mechanisms, Physicochemical Changes, Assessment, And Implications for Field Applications. *Environ. Sci. Technol.* **2020**, *54*, 14797–14814. [CrossRef] [PubMed]
50. Zimmerman, A.R.; Gao, B.; Ahn, M.-Y. Positive and negative carbon mineralization priming effects among a variety of biochar-amended soils. *Soil Biol. Biochem.* **2011**, *43*, 1169–1179. [CrossRef]
51. Zhang, Y.; Hou, R.; Fu, Q.; Li, T.; Li, M.; Dong, S.; Shi, G. Soil environment, carbon and nitrogen cycle functional genes in response to freeze-thaw cycles and biochar. *J. Clean. Prod.* **2024**, *444*, 141345. [CrossRef]
52. Gao, D.; Bai, E.; Yang, Y.; Zong, S.; Hagedorn, F. A global meta-analysis on freeze-thaw effects on soil carbon and phosphorus cycling. *Soil Biol. Biochem.* **2021**, *159*, 108283. [CrossRef]
53. Zhu, L.; Chen, N.; Zhang, X.; Ren, L.; Zou, R.; Xie, J.; Wang, Z.; Yang, H.; Hao, Z.; Qin, J.; et al. Freeze–Thaw Cycle Events Enable the Deep Disintegration of Biochar: Release of Dissolved Black Carbon and Its Structural-Dependent Carbon Sequestration Capacity. *Environ. Sci. Technol.* **2024**, *58*, 20979–20989. [CrossRef]
54. Kong, F.; Gao, Y.; Li, T.; Fu, Q.; Liu, D.; Su, Z.; Shen, W.; Wang, J.; Zhou, W.; Wang, Y. Effects of freeze–thaw cycles and the soil water content on carbon and nitrogen changes in different soil types of Heilongjiang Province, China. *Soil Use Manag.* **2023**, *39*, 1453–1466. [CrossRef]
55. de Bruijn, A.M.G.; Butterbach-Bahl, K.; Blagodatsky, S.; Grote, R. Model evaluation of different mechanisms driving freeze–thaw N2O emissions. *Agric. Ecosyst. Environ.* **2009**, *133*, 196–207. [CrossRef]
56. Sawicka, J.E.; Robador, A.; Hubert, C.; Jørgensen, B.B.; Brüchert, V. Effects of freeze–thaw cycles on anaerobic microbial processes in an Arctic intertidal mud flat. *ISME J.* **2010**, *4*, 585–594. [CrossRef] [PubMed]
57. Patel, K.F.; Tatariw, C.; MacRae, J.D.; Ohno, T.; Nelson, S.J.; Fernandez, I.J. Repeated freeze–thaw cycles increase extractable, but not total, carbon and nitrogen in a Maine coniferous soil. *Geoderma* **2021**, *402*, 115353. [CrossRef]
58. Nguyen, T.T.N.; Xu, C.-Y.; Tahmasbian, I.; Che, R.; Xu, Z.; Zhou, X.; Wallace, H.M.; Bai, S.H. Effects of biochar on soil available inorganic nitrogen: A review and meta-analysis. *Geoderma* **2017**, *288*, 79–96. [CrossRef]
59. Cayuela, M.L.; Spott, O.; Pascual, M.B.; Sánchez-García, M.; Sánchez-Monedero, M.A. Key biochar properties linked to denitrification products in a calcareous soil. *Biochar* **2024**, *6*, 90. [CrossRef]
60. Pan, Y.; She, D.; Shi, Z.; Cao, T.; Xia, Y.; Shan, J. Salinity and high pH reduce denitrification rates by inhibiting denitrifying gene abundance in a saline-alkali soil. *Sci. Rep.* **2023**, *13*, 2155. [CrossRef]
61. Jindo, K.; Audette, Y.; Higashikawa, F.S.; Silva, C.A.; Akashi, K.; Mastrolonardo, G.; Sánchez-Monedero, M.A.; Mondini, C. Role of biochar in promoting circular economy in the agriculture sector. Part 1: A review of the biochar roles in soil N, P and K cycles. *Chem. Biol. Technol. Agric.* **2020**, *7*, 15. [CrossRef]
62. Ji, X.; Liu, M.; Yang, J.; Feng, F. Meta-analysis of the impact of freeze–thaw cycles on soil microbial diversity and C and N dynamics. *Soil Biol. Biochem.* **2022**, *168*, 108608. [CrossRef]

63. Lv, H.; Ji, C.; Zhang, L.; Jiang, C.; Cai, H. Zinc application promotes nitrogen transformation in rice rhizosphere soil by modifying microbial communities and gene expression levels. *Sci. Total Environ.* **2022**, *849*, 157858. [CrossRef]
64. Rodríguez-Berbel, N.; Ortega, R.; Lucas-Borja, M.E.; Solé-Benet, A.; Miralles, I. Long-term effects of two organic amendments on bacterial communities of calcareous mediterranean soils degraded by mining. *J. Environ. Manag.* **2020**, *271*, 110920. [CrossRef]
65. Li, Y.; Ling, W.; Yang, J.; Xing, Y.; Zhang, Q.; Feng, L.; Hou, J.; Hou, C.; Lu, Q.; Wu, T.; et al. Study on the impact of microplastic characteristics on ecological function, microbial community migration and reconstruction mechanisms during saline-alkali soil remediation. *J. Hazard. Mater.* **2025**, *495*, 139044. [CrossRef]
66. Geng, S.; Cao, W.; Yuan, J.; Wang, Y.; Guo, Y.; Ding, A.; Zhu, Y.; Dou, J. Microbial diversity and co-occurrence patterns in deep soils contaminated by polycyclic aromatic hydrocarbons (PAHs). *Ecotoxicol. Environ. Saf.* **2020**, *203*, 110931. [CrossRef]
67. Suyal, D.C.; Joshi, D.; Kumar, S.; Soni, R.; Goel, R. Differential protein profiling of soil diazotroph Rhodococcus qingshengii S10107 towards low-temperature and nitrogen deficiency. *Sci. Rep.* **2019**, *9*, 20378. [CrossRef]
68. Chen, X.; Shan, G.; Shen, J.; Zhang, F.; Liu, Y.; Cui, C. In situ bioremediation of petroleum hydrocarbon–contaminated soil: Isolation and application of a Rhodococcus strain. *Int. Microbiol.* **2022**, *26*, 411–421. [CrossRef]
69. Lan, J.; Wang, S.; Wang, J.; Qi, X.; Long, Q.; Huang, M. The Shift of Soil Bacterial Community After Afforestation Influence Soil Organic Carbon and Aggregate Stability in Karst Region. *Front. Microbiol.* **2022**, *13*, 901126. [CrossRef]
70. Zhang, Y.-G.; Chen, J.-Y.; Wang, H.-F.; Xiao, M.; Yang, L.-L.; Guo, J.-W.; Zhou, E.-M.; Zhang, Y.-M.; Li, W.-J. Egicoccus halophilus gen. nov., sp. nov., a halophilic, alkalitolerant actinobacterium and proposal of Egicoccaceae fam. nov. and Egicoccales ord. nov. *Int. J. Syst. Evol. Microbiol.* **2016**, *66*, 530–535. [CrossRef]
71. Kasana, R.C.; Pandey, C.B. Exiguobacterium: An overview of a versatile genus with potential in industry and agriculture. *Crit. Rev. Biotechnol.* **2017**, *38*, 141–156. [CrossRef] [PubMed]